Acylsugars Protect Nicotiana Benthamiana Against Insect Herbivory and Desiccation

Honglin Feng
Boyce Thompson Institute for Plant Research
Lucia Acosta-Gamboa
Cornell University
Lars H Kruse
Cornell University
Jake D Tracy
Cornell University
Seung Ho Chung
Boyce Thompson Institute for Plant Research
Alba Ruth Nava Fereira
The University of Texas at San Antonio
Sara Shakir
Boyce Thompson Institute for Plant Research
Hongxing Xu
Boyce Thompson Institute for Plant Research
Garry Sunter
The University of Texas at San Antonio
Michael A Gore
Cornell University
Clare L Casteel
Cornell University
Gaurav D. Moghe
Cornell University
Georg Jander (gj32@cornell.edu)
Boyce Thompson Institute For Plant Research https://orcid.org/0000-0002-9675-934X

Research Article

Keywords: acylsugar, aphid, ASAT, desiccation, Nicotiana benthamiana, whitefly

Posted Date: June 15th, 2021

DOI: https://doi.org/10.21203/rs.3.rs-596878/v1

Article Title

Acylsugars protect *Nicotiana benthamiana* against insect herbivory and desiccation

Author names

Honglin Feng[a], Lucia Acosta-Gamboa[b], Lars H. Kruse[c,f], Jake D. Tracy[d,g], Seung Ho Chung[a], Alba Ruth Nava Fereira[e], Sara Shakir[a,h], Hongxing Xu[a,i], Garry Sunter[e], Michael A. Gore[b], Clare L. Casteel[d], Gaurav D. Moghe[c], Georg Jander[a*]

Author Affiliations

[a]Boyce Thompson Institute, Ithaca NY, USA
[b]Plant Breeding and Genetics Section, School of Integrative Plant Science, Cornell University, Ithaca NY, 14853, USA
[c]Plant Biology Section, School of Integrative Plant Science, Cornell University, Ithaca NY, 14853, USA
[d]Plant-Microbe Biology and Plant Pathology Section, School of Integrative Plant Science, Cornell University, Ithaca NY, 14853, USA
[e]Department of Biology, University of Texas San Antonio, San Antonio TX, 78249, USA
[f]Present address: Michael Smith Laboratories, University of British Columbia, Vancouver, BC, V6T 1Z4, Canada
[g]Present address: Department of Plant Sciences & Plant Pathology, Montana State University, Bozeman MT, 59717, USA
[h]Present address: Gembloux Agro-Bio Tech Institute, the University of Liege, Gembloux, Belgium
[i]Present address: College of Life Science, the Shaanxi Normal University, Xi'an, China

***Correspondence:**

Georg Jander
Boyce Thompson Institute
Ithaca, NY 14853
USA
Phone: 607-254-1365
Email: gj32@cornell.edu
ORCID: 0000-0002-9675-934X

Key Message:

Nicotiana benthamiana acylsugar acyltransferase (ASAT) is required for protection against desiccation and insect herbivory, and knockout mutations provide a new resource for investigation of plant-aphid and plant-whitefly interactions.

Abstract

Nicotiana benthamiana is used extensively as a transient expression platform for functional analysis of genes from other species. Acylsugars, which are produced in the trichomes, are a hypothesized cause of the relatively high insect resistance that is observed in *N. benthamiana.* We characterized the *N. benthamiana* acylsugar profile, bioinformatically identified two acylsugar acyltransferase genes, *ASAT1* and *ASAT2*, and used CRISPR/Cas9 mutagenesis to produce acylsugar-deficient plants for investigation of insect resistance and foliar water loss. Whereas *asat1* mutations reduced accumulation, *asat2* mutations caused almost complete depletion of foliar acylsucroses. Three hemipteran and three lepidopteran herbivores survived, gained weight, and/or reproduced significantly better on *asat2* mutants than on wildtype *N. benthamiana*. Both *asat1* and *asat2* mutations reduced the water content and increased leaf temperature. Our results demonstrate the specific function of two ASAT proteins in *N. benthamiana* acylsugar biosynthesis, insect resistance, and desiccation tolerance. The improved growth of aphids and whiteflies on *asat2* mutants will facilitate the use of *N. benthamiana* as a transient expression platform for the functional analysis of insect effectors and resistance genes from other plant species. Similarly, the absence of acylsugars in *asat2* mutant*s* will enable analysis of acylsugar biosynthesis genes from other Solanaceae by transient expression.

Keywords: acylsugar, aphid, ASAT, desiccation, *Nicotiana benthamiana*, whitefly

Introduction

Nicotiana benthamiana, a wild tobacco species that is native to Australia, is commonly employed by plant molecular biologists as platform for investigating plant-virus interactions (Goodin et al., 2008), expression of transgenes using viral and bacterial vectors (Bally et al., 2018), and overproducing proteins and small molecules for subsequent purification (Arntzen, 2015; Powell, 2015). Although *N. benthamiana* has been used extensively for studying plant-virus and plant-bacterial interactions, is not a very suitable host for tobacco feeding generalist herbivores, in particular Hemiptera such as *Myzus persicae* (green peach aphid; Thurston, 1961; Hagimori et al., 1993) and *Bemisia tabaci* (whitefly; Simon et al., 2003).

The poor growth of generalist insect herbivores on *N. benthamiana* may be attributed in part to glandular trichomes. These epidermal secretory structures on the leaf surface of ~30% of vascular plants (Weinhold and Baldwin, 2011; Glas et al., 2012) have been found to play a crucial defensive role in several ways: as a physical obstacle for insect movement (Cardoso, 2008), entrapment (Simmons et al., 2004), synthesis of volatiles and defensive metabolites (Laue et al., 2000; Schilmiller et al., 2010; Glas et al., 2012), and production of herbivore-resistant proteins (e.g. T-phylloplanin; Shepherd and Wagner, 2007). In addition, glandular trichomes also protect plants from abiotic stresses like transpiration water loss and UV irradiation (Karabourniotis et al., 1995).

There are two main types of glandular trichomes on *N. benthamiana* leaves, large swollen-stalk trichomes and small trichomes that are capped by a secretory head with one, two, or four cells. The large trichomes have been shown to secrete phylloplane proteins in *N. tabacum*. The small trichomes, which are the most abundant on tobacco leaf surfaces, secrete exudates, including acylsugars (Wagner et al., 2004; Slocombe et al., 2008).

Acylsugars, generally sucrose or glucose esterified with aliphatic acids of different chain lengths (Fig. **1**), are abundant insect-deterrent metabolites (Arrendale et al., 1990; Slocombe et al., 2008; Moghe et al., 2017). Specific acylsugars, which were associated with aphid-resistant *Nicotiana* species, were not detected in susceptible species in this genus (Hagimori et al., 1993). Relative to cultivated tomatoes (*Solanum lycopersicum*), acylsugars found in wild tomatoes (*Solanum pennellii*) were associated with greater resistance against *M. persicae* and *B. tabaci* (Rodriguez et al., 1993; Marchant et al., 2020). The synthetic sucrose octanoate (an analog of *Nicotiana gossei* sugar esters) was effective in the field against Asian citrus psyllids (*Diaphorina citri*), citrus leafminer (*Phyllocnistis citrella*), and a mite complex (including Texas citrus mite, red spider mite, and rust mite) (McKenzie and Puterka, 2004; McKenzie et al., 2005).

Acylsugars and leaf surface lipids more generally may contribute to plant drought tolerance. Transcriptomic studies of drought-tolerant *S. pennellii* populations showed that lipid metabolism genes

were among those that are most responsive to drought stress (Gong et al., 2010; Egea et al., 2018), and high acylsugar abundance was associated with drought tolerance (Fobes et al., 1985). Similarly, acylsugar abundance was correlated with drought tolerance in *Solanum chilense* (O' Connell et al., 2007) and *Nicotiana obtusifolia* (Kroumova et al., 2016). Although the mechanism is not completely understood, it has been proposed that the polar lipids reduce the surface tension of adsorbed dew water, thereby allowing the leaves absorb more condensed water (Fobes et al., 1985).

Recently, enzymes involved in acylsugar biosynthesis have been identified. Four acylsugar acyltransferases (ASATs), *Sl*ASAT1, *Sl*ASAT2, *Sl*ASAT3, and *Sl*ASAT4, have been biochemically characterized in cultivated tomato (Fan et al., 2016). *Sl*ASAT1 catalyzes the first step of sucrose acylation, using sucrose and acyl-CoA to generate monoacylsucroses via pyranose R_4 acylation. *Sl*ASAT2 uses the product of *Sl*ASAT1 and acyl-CoA to generate diacylsucroses. Further, *Sl*ASAT3 uses the diacylsucroses generated by *Sl*ASAT2 to make triacylsucroses by acylating the diacylsucrose five-membered (furanose) ring (Fan et al., 2016). Then, *Sl*ASAT4 (formerly *Sl*ASAT2), specifically expressed in the trichomes, makes tetraacylsucroses by acetylating triacylsucroes using C2-CoA (Schilmiller et al., 2012). The expression, activity, and even the order of ASATs in the biosynthetic pathway varies among different plant species, which likely contributes to the observed trichome chemical diversity (Kim et al., 2012).

ASATs have been studied most intensively in tomato, and are annotated in other available *Nicotiana* genomes (Gaquerel et al., 2013; Van et al., 2017; Egan et al., 2019). However, *ASAT* genes in *N. benthamiana* were not previously annotated or functionally characterized. Therefore, the goal of current study was to investigate the role of acylsugars in protecting *N. benthamiana* against insect feeding and foliar water loss, as well as to create an insect-susceptible *ASAT* mutant line to facilitate use of *N. benthamiana* for research on plant-insect interactions. We bioinformatically identified two *ASAT* genes in *N. benthamiana*, *NbASAT1* and *NbASAT2*. Using CRISPR/Cas9 to create *NbASAT1* and *NbASAT2* mutant lines, we showed that knockout mutations reduced acylsugar content, decreased resistance to six generalist insect herbivores [*M. persicae*, *B. tabaci, Macrosiphum euphorbiae* (potato aphid), *Helicoverpa zea* (corn earworm), *Heliothis virescens* (tobacco budworm), and *Trichoplusia ni* (cabbage looper)], and increased foliar water loss

Results

Identification of ASAT1 *and* ASAT2 *in N. benthamiana*

Using reciprocal comparisons to confirmed Solanaceae *ASAT* genes (Moghe et al., 2017), we identified three highly homologous sequences in the *N. benthamiana* genome: Niben101Scf02239Ctg025, Niben101Scf22800Ctg001, and Niben101Scf14179Ctg028 (gene identifiers are from annotations at

solgenomics.net) (Bombarely et al., 2012). Whereas Niben101Scf02239Ctg025 and Niben101Scf22800Ctg001 were annotated as a full-length coding sequences with strong coverage in available RNAseq datasets, Niben101Scf14179Ctg028 was annotated as a pseudogene because it appears to be a fragment of the predicted cDNA Niben101Scf141790g02010.1 with no coverage in available RNAseq datasets. In a more recently assembled *N. benthamiana* genome (Schiavinato et al., 2019), the Niben101Scf02239Ctg025 and Niben101Scf22800Ctg001 sequences were confirmed, the pseudogene Niben101Scf14179Ctg028 was annotated as part of Niben101Scf02239Ctg025, and there were no additional annotated ASAT candidates.

To infer ASAT evolution and function, we constructed a protein phylogenetic tree of previously annotated Solanaceae ASATs (Figs. **2, S1, S2**; Tables **S1, S2**). In this tree, Niben101Scf02239Ctg025 formed a monophyletic group with other ASATs including the biochemically characterized *Ss*ASAT1, *Pa*ASAT1 and *Hn*ASAT1. Therefore, we named Niben101Scf02239Ctg025 as *N. benthamiana* ASAT1 (*Nb*ASAT1). Niben101Scf22800Ctg001 formed a monophyletic group with other ASATs including the biochemically characterized *Na*ASAT2, *Hn*ASAT2, and *Pa*ASAT2. Therefore, we named Niben101Scf22800Ctg001 as *N. benthamiana* ASAT2 (*Nb*ASAT2). Notably, the ASAT2 monophyletic group also included the biochemically characterized *Sp*ASAT1, *Sl*ASAT1, and *Sn*ASAT1 (Fig. **2**).

Generation of ASAT *mutants*

Using CRISPR/Cas9 coupled with tissue culture, we obtained two independent homozygous mutants for both *NbASAT1* and *NbASAT2*. *asat1-1* has a five-nucleotide deletion at the gRNA3 cutting site and a single-nucleotide insertion at the gRNA2 cutting site, leading to a frameshift between gRNA3 and gRNA2. *asat1-2* has a 318-nucleotide deletion between the gRNA3 and gRNA2 cutting sites (Fig. **3**a). *asat2-1* has a single-nucleotide deletion at the gRNA3 cutting site and single-nucleotide insertion at the gRNA2 cutting site, leading to a frameshift between the two sites. *asat2-2* has a 115-nucleotide deletion at the gRNA3 cutting site and a single-nucleotide insertion at the gRNA2 cutting site (Fig. **3b**).

Even though *ASAT1* and *ASAT2* are located on different scaffolds in the *N. benthamiana* genome assembly (Schiavinato et al., 2019), we were not able to find homozygous *asat1 asat2* double mutants among 40 F2 progeny from crosses between *asat1* and *asat2* plants. Similarly, when we transformed *N. benthamiana* in tissue culture with gRNA targeting both *ASAT1* and *ASAT2*, simultaneously or sequentially, we identified each individual knockout mutation, but no homozygous double mutants. Although we cannot completely rule out other scenarios, it is possible that *asat1 asat2* double mutations are deleterious or lethal for *N. benthamiana.*

ASAT2 *knockout depletes acylsugar biosynthesis*

In the LC/MS profile of *N. benthamiana* leaf surface washes, we characterized twelve mass features as acylsucroses based on their characteristic peaks and neutral losses. Those twelve *m/z* ratios included 383.12, 467. 21, 509.22, 555.23, 593.32, 621.31, 625.31, 635.32, 639.32, 667.32, 671.30, 681.34 (Fig. **S3a**). In negative electron spray ionization mode, the characteristic peak features included *m/z* of 341.11 for sucrose, 509.22 for sucrose+C2+C8, 467.21 for sucrose+C8, 495.21 for sucrose+C7, and 383.12 for sucrose+C2; the neutral loss peaks included mass for 126.10 for C8 (acyl-chain with 8 carbons), 129.09 for C7+H_2O, and 59.01 for C2+H_2O (Fig. **S3b**). Based on their MS/MS peak features, retention times and relative abundances, we predicted that the identified mass features are mainly derived from two acylsucroses as formate or chloride adducts, pathway intermediates, and/or resulted from in-source fragmentation. We named the two acylsucroses S3:17(2,7,8) and S3:18(2,8,8) (in the nomenclature, "S" refers to the sucrose backbone, "3:18" indicates three acyl chains with total eighteen carbons, and the length of each acyl chain is shown in parentheses) (Fig. **1**; **S3a**).

In wildtype plants, S3:18(2,8,8) is the dominant acylsucrose, whereas S3:17(2,7,8) has relatively low abundance (Fig. **4**). S2:16(8,8) and S2:15(7,8), which may be biosynthetic pathway intermediates for S3:18(2,8,8) and S3:17(2,7,8), respectively, are present at lower levels. Compared to wildtype *N. benthamiana*, both *asat2-1* and *asat2-2* were almost completely depleted in both S3:17(2,7,8) and S3:18(2,8,8), as well as in the two predicted biosynthetic intermediates S2:15(7,8) and S2:16(8,8). For *asat1-1* and *asat1-2*, the detected acylsucroses were less abundant and significantly reduced only in *asat1-1* (Fig. **4**). Although acylsugar content was reduced in the *ASAT* mutants, the structure and abundance of trichomes on the leaf surface were not visibly changed (Fig. **S4**).

Insect performance is improved on* ASAT2 *mutant lines

To test the role of acylsugars in protecting *N. benthamiana* against insect pests, we started with synchronized first-instar *M. persicae* to monitor aphid survival and growth over time. Significant improvements in aphid survivorship were observed as early as at 2 days post-feeding ($p < 0.001$) on the *asat2-1* and *asat2-2* mutants and increased until the end of the 5-day monitoring period ($p < 0.001$) (Fig. **5a**; Table **S3**). After 5 days of feeding, surviving aphids on both *asat1* and *asat2* plants were larger than those on wildtype plants (Fig. **5b**). When we measured progeny production by five adult aphids over a period of seven days, an average of more than 200 nymphs were produced on the *asat2* mutants, significantly more than the number of nymphs produced on either wildtype or *asat1* mutants ($p < 0.05$, Fig. **5c**). In aphid choice assays, a preference for *asat2-1* and *asat2-2* leaves was consistently observed in any pairwise combination with wildtype, *asat1-1*, and *asat1-2* leaves ($p < 0.001$, *Chi-square* test, Fig. **5d,e; S5**). No *M. persicae* preference was observed between wildtype *N. benthamiana* and *asat1* mutants ($p > 0.05$, Fig. **5f; S5**).

When aphid colonies were allowed to grow long-term on *asat2-1* mutant and wildtype *N. benthamiana* in the same cage, there were many more aphids on the mutant plants (Fig. **S6a,b**), likely resulting from a combination of host plant choice and increase growth on the *asat2-1* mutant. It is noteworthy that, on the *asat2-1* mutant plants, aphids were feeding on the more nutritious younger leaves, which tend to be better-defended in plants. By contrast, on wildtype *N. benthamiana* aphids were only were able to feed on older, senescing leaves and were primarily on the abaxial surface. Consistent with the increased aphid presence, growth of the *asat2-1* mutant plants were visibly reduced relative to wildtype *N. benthamiana* (Fig. **S6b**). Given the almost identical phenotypes of *asat2-1* and *asat2-2* mutants, subsequent insect assays were conducted with T2 progeny of the *asat2-1* line.

As we observed with *M. persicae*, the *asat2-1* mutation improved *M. euphorbiae* performance on *N. benthamiana* (Fig. **6a-c**). Significantly increased *M. euphorbiae* survival was observed after 24 h on *asat2-1* compared to wildtype ($p < 0.001$, Fig. **6a**). Additionally, significantly more nymphs were produced by adult *M. euphorbiae* in the course of 24 h on *asat2-1* than on wildtype ($p < 0.05$, Fig. **6b**). In choice assays, potato aphids preferentially chose *asat2-1* leaves over wildtype leaves ($p < 0.001$, Fig. **6c**). Whereas we were not able to establish an *M. euphorbiae* colony on wildtype *N. benthamiana*, the aphids readily formed colonies on the *asat2-1* mutant plants (Fig. **6d**).

Survival of *B. tabaci* adults was greatly increased on the *asat2-1* mutant relative to wildtype *N. benthamiana* (Fig. **6e**). Moreover, *whiteflies* laid significantly fewer eggs on wildtype than on *asat2-1* mutant plants over three days (Fig. **6f**). Dead adult whiteflies were observed on wildtype plants (Fig. **S7a**), and it was not possible to establish a reproducing colony. By contrast, after 23 days of feeding, whiteflies of different life stages were observed on *asat2-1* mutant plants (Fig. **S7b-d**). In choice assays with mutant and wildtype plants in the same cage, whiteflies preferentially settled on *asat2-1* plants (72%) over wildtype (26%) in a 24-h experiment (Fig. **6g**). Notably, after 24 h, all whiteflies on *asat2-1* were alive, whereas about half of the whiteflies that had settled on the wildtype plants were dead (Fig. **6f**).

To determine whether depletion of acylsugars in *ASAT2* mutants improves the performance of generalist lepidopteran herbivores on *N. benthamiana*, we conducted experiments with *H. zea*, *H. virescens*, and *T. ni*. When neonates were placed on the leaves of wildtype or *asat2-1* mutant, no *H. zea* caterpillars were recovered (Fig. **7a**). Survivorship of *H. virescens* and *T. ni* larvae on *N. benthamiana* was low, and the mass of the surviving larvae after ten days was not significantly increased on the mutant relative to wildtype (Fig. **7b,c**). Due to the low survival of neonates, we repeated the caterpillar bioassay using five-day-old larvae that had been reared on artificial diet. Almost all *H. zea* and *H. virescens* larvae survived for seven days on wildtype and *asat2-1* mutant plants, and survival of *T. ni* caterpillars was higher on *asat2-1* than on wildtype plants (Fig. **7d-f**). The relative growth rates of surviving *H. zea*, *H.*

virescens, and *T. ni* larvae were higher on the *asat2-1* mutant by 35%, 47%, and 99%, respectively, than on wildtype plants (Fig. **7d-f**).

Water loss is greater in* asat2 *mutant plants than in wildtype

While conducting aphid choice assays with detached leaves (Fig. **5d-f; 6c**), we noticed that the mutant leaves dried out faster than wildtype leaves. This effect was quantified using detached-leaf assays, in which *asat2* leaves lost significantly more water over 24 h than leaves from either wildtype or *asat1* mutant (Fig. **8a; S8a**). Using hyperspectral imaging, we determined that the leaf water content of intact plants, as measured by the water band index (WBI), was significantly lower in *asat2* mutants than in wildtype (Fig. **8b; S8b**). Although the *asat1* mutants did not lose water faster than wildtype in detached leaf assays (Fig. **8a**), the leaf water content in *asat1* mutants was significantly lower than wildtype (Fig. **8b; S8b**). Measurement of leaf temperature by thermal imaging showed that, consistent with the reduced leaf water content, the leaf temperature of the acylsugar mutants was significantly higher than that of wildtype plants (Fig. **8c; S8c**).

Discussion

We identified only two *ASAT* genes, *NbASAT1* and *NbASAT2*, and a fragmented pseudogene, in the *N. benthamiana* genome (Table **S2**). By contrast, in other *Nicotiana* species, there are more predicted *ASATs*, *e.g.* one *ASAT1*, one *ASAT2*, and 20 *ASAT3*-like genes in *N. attenuata* (Gaquerel et al., 2013; Van et al., 2017), 35 *ASAT3*-like genes in *N. tabacum*, and 19 *ASAT3*-like genes in *N. tomentosiformis* (Egan et al., 2019). Given the small number of predicted *ASAT* genes in *N. benthamiana*, other enzymes may also be involved in acylsugar biosynthesis. For instance, knockdown of *E1-β branched-chain α-keto acid dehydrogenase* significantly reduces acylsugars in *N. benthamiana* (Slocombe et al., 2008). Additionally, *Isopropylmalate Synthase 3* in cultivated and wild tomatoes (Ning et al., 2015) and *Acyl-Sucrose Fructo-Furanosidase 1* in wild tomato (Leong et al., 2019) encode enzymes that are involved in determining acylsugar composition. Further studies will be needed to characterize other genes involved in *N. benthamiana* acylsugar biosynthesis.

Acylsugars can be categorized as sucrose or glucose esters based on the sugar cores, which are decorated with varying numbers or lengths of acyl chains (Kim et al., 2012). Whereas some wild tomatoes produce a mixture of acylsucroses and acylglucoses, we observed only acylsucroses (Fig. **1; 4**), consistent with previous identification of these compounds in *N. benthamiana* (Matsuzaki et al., 1989; Matsuzaki et al., 1992; Hagimori et al., 1993; Slocombe et al., 2008). Nevertheless, it has been reported that *N. benthamiana* produces acylglucoses, although in lower abundance than acylsucroses (Hagimori et al., 1993), and one acylglucose structure has been proposed (Matsuzaki et al., 1992). Our failure to detect

acylglucoses may be explained by the use of different isolates of *N. benthamiana*, growth conditions, plant stage, and/or the detection methods. Whereas we used ~1-month-old plants and LC/MS, Matsuzaki et al. (1992) used ~3-month-old plants and GC/MS to detect acylglucoses in *N. benthamiana*.

The abundance of the characterized acylsugars was reduced to a greater extent in *N. benthamiana asat2* than in *asat1* mutants (Fig. **4**). This suggests that either *Nb*ASAT2 functions upstream of *Nb*ASAT1 in the acylsugar biosynthesis pathway, but partially complements *Nb*ASAT1 activity, or *Nb*ASAT1 and *Nb*ASAT2 have similar functions in the biochemical pathway, but *NbASAT2* had higher abundance or enzymatic activity. It is not known whether *N. benthamiana* ASATs are monomeric or multimeric, but BAHD acyltransferases generally are monomeric enzymes (D'Auria, 2006), suggesting that heterodimers between ASAT1 and ASAT2 are unlikely to affect the observed phenotypes.

In the ASAT phylogenetic tree (Fig. **2**), *Nb*ASAT2 is closely related to some biochemically characterized ASAT1 proteins in other Solanaceae species, including the *Sp*ASAT1, *Sl*ASAT1, and *Sn*ASAT1. Those ASAT1s have some substrate overlap with the ASAT2s found in the corresponding species, indicating that ASAT2 has moved toward utilizing the ASAT1 substrate in these species over time (Moghe et al., 2017). The final activity shift that has become fixed in the *Solanum* genus, most likely occurred after the divergence of the *Solanum* and *Capsicum* clades (Moghe et al., 2017). However, if our hypothesis of partial complementation of *Nb*ASAT1 by *Nb*ASAT2 is correct, it may flag a transition stage or suggest independent *Nicotiana*-specific evolution of the ASAT1 and ASAT2 functions. Based on previous knowledge of BAHD activities (Moghe et al., 2017), we postulate that S2:15 (7,8) and S2:16 (8,8) are produced by *Nb*ASAT1 and *Nb*ASAT2, whereas the acetylation is carried out by another unrelated BAHD enzyme – not unlike the distantly related *Sl*ASAT4 and *Salpiglossis sinuata* ASAT5 (Schilmiller et al., 2015; Moghe et al., 2017). Further characterization will be required to identify specific acyltransferase activities in *N. benthamiana*.

The observed role of acylsugars in protecting against desiccation (Fig. **8; S8**) is consistent with reports from other Solanaceae (Fobes et al., 1985; O' Connell et al., 2007; Kroumova et al., 2016), though this has not previously been verified with isogenic mutant and wildtype plants. In *N. benthamiana*, the drought-protective function of acylsugars is likely an adaptation to the seasonally arid native habitat in northwestern Australia (Goodin et al., 2008; The Australasian Virtual Herbarium, https://avh.ala.org.au). Relative to *asat1* mutants, the lower acylsugar content of *asat2* mutants (Fig. **4**), resulted in more rapid water loss in detached leaves (Fig. **8a; S8a**). However, despite the only partial decrease in the acylsugar content of *asat1* mutants, the decreases in water content and increases in leaf temperature of intact plants were similar to those of *asat2* mutants (Fig. **8b,c; S8b,c**).

Acylsugars with $C_{7\text{-}12}$ chains have been shown to be the most toxic sugar esters for small phloem-feeding Hemiptera such as aphids, Asian citrus psyllids, and whiteflies (Chortyk et al., 1996; McKenzie

and Puterka, 2004; Song et al., 2006). Synthetic acylsucroses with di-heptanoic acid (C7), di-octanoic acid (C8), and di-nonanoic acid (C9) acyl groups showed the highest mortality in bioassays with *M. persicae* and *B. tabaci* (Chortyk et al., 1996; McKenzie and Puterka, 2004; Song et al., 2006). *Nicotiana gossei*, a tobacco species that produces mainly C7-C8 acyl group acylsugars, has a high level of insect resistance relative to close relatives with acylsugar profiles that are not dominated by those with C7-C12 acyl groups (Thurston, 1961; Kroumova and Wagner, 2003). In *N. benthamiana*, the two most abundant acylsugars that we found contain C7 and predominantly C8 acyl groups, which is consistent with previous findings of mainly 5- and 6-methyl heptanoate (C8) in *N. benthamiana* (Kroumova and Wagner, 2003; Slocombe et al., 2008) and *N. alata* (Moghe et al., 2017). The almost complete depletion of acylsugars in our *asat2* mutants improved both hemipteran and lepidopteran performance, suggesting that the identified C8 acyl group acylsugars are providing insect resistance for *N. benthamiana*.

We cannot rule out the possibility of secondary effects that might also influence insect performance on acylsugar-depleted *N. benthamiana*. Specialized metabolites in other plants, for instance glucosinolates in *Arabidopsis thaliana* (Clay et al., 2009) and benzoxazinoids in *Zea mays* (Meihls et al., 2013), regulate callose deposition as a secondary defense response. It is not known whether acylsugars contribute to the regulation of other defense responses in *N. benthamiana.* The observation of numerous dead whiteflies on wildtype *N. benthamiana* plants in choice assays (Fig. **6g**), despite the option of moving to presumably more desirable *asat2-1* mutant plants in the same cage, suggests that the acylsugars stickiness also plays a role in plant defense by immobilizing the insects. Both altered leaf turgor and leaf temperature (Fig. **8b,c**) could affect insect feeding behavior and growth rate, though the specific effects on the six tested insect species cannot be determined without further research.

Although *H. zea*, *H. virescens*, and *T. ni* larvae grow well on cultivated tobacco, neonate larvae had a low survival rate on both wildtype and *asat2-1 N. benthamiana* (Fig. **7a-c**). There was a higher survival rate with five-day-old larvae of the three tested species, which all grew significantly better on *asat2-1* mutants than on wildtype *N. benthamiana* (Fig. **7d-f**). Thus, *N. benthamiana* acylsugars likely provide at least some protection against lepidopteran pests. However, the high mortality of neonate larvae on *asat2-1* plants suggests that either residual acylsugars or as yet unknown resistance mechanisms in *N. benthamiana* can provide protection. Additional mutations that decrease insect resistance, perhaps regulatory genes such as *COI1* or genes affecting the production of other specialized metabolites, will be necessary to facilitate *N. benthamiana* experiments with *H. zea*, *H. virescens*, *T. ni*, and other commonly studied lepidopteran species.

The high mortality of hemipteran pests such as *M. persicae* and *B. tabaci* on wildtype *N. benthamiana* (Fig. **5, 6**) makes it challenging to interpret insect bioassays involving the transient expression of heterologous genes. Our knockout of acylsugar biosynthesis is an important step toward

making the already excellent *N. benthamiana* model system (Goodin et al., 2008; Bally et al., 2018) more suitable for studying plant-insect interactions. Future plant-insect interactions research using *asat2* mutant plants may include: (i) functional analysis of additional *N. benthamiana* genes in the *asat2* mutant background by CRISPR/Cas9 mutagenesis using a newly developed virus-mediated gRNA delivery system (Ellison et al., 2020), (ii) transient expression assays to test the function of both insect-produced elicitors and insect-defensive genes from other plant species in *N. benthamiana asat2* mutants (Bos et al., 2010; Casteel et al., 2014; Elzinga et al., 2014; Rodriguez et al., 2014), and (iii) virus-induced gene silencing (VIGS) to down-regulate gene expression in insects feeding on *N. benthamiana* (Feng and Jander, 2021). Furthermore, the almost complete absence of acylsugars in the *asat2* mutant lines, coupled with the facile *Agrobacterium* and virus-mediated transient gene expression systems that are available for *N. benthamiana*, will make these mutants a suitable platform for the functional analysis of ASATs from other Solanaceae.

Materials and Methods

Insect and plant cultures

A tobacco-adapted red strain of *M. persicae* (Ramsey et al., 2007; Ramsey et al., 2014) was maintained on *N. tabacum* plants in a growth room at 23°C with a 16:8 h light:dark photoperiod. A colony of *B. tabaci* MEAM1 were provided by Jane Polston (University of Florida) and was maintained on tobacco (*Nicotiana tabacum*). *Macrosiphum euphorbiae* was obtained from Isgouhi Kaloshian (UC Riverside) and was maintained on tomato (*Solanum lycopersicum*) cv. Moneymaker. Eggs of *H. zea*, *H. virescens*, and *T. ni* were purchased from Benzon Research (www.benzonresearch.com). *Nicotiana benthamiana* wild type and mutant plants for aphid experiments, caterpillar experiments were maintained at 23°C and a 16:8 h light:dark photoperiod in a Conviron (Winnipeg, Canada) growth chamber and, for seed production, in a greenhouse at 27/24°C (day/night) with ambient light conditions. Wild type and mutant *N. benthamiana* plants for whitefly choice and no-choice assays were maintained at 26°C and a 16:8 h light:dark photoperiod in a growth room.

Identification of ASAT1 and ASAT2 orthologs in N. benthamiana

To identify ASAT1 and ASAT2 orthologs in *N. benthamiana*, protein sequences of *Salpiglossis sinuata* and *Solanum lycopersicum* ASAT1 and ASAT2 (Moghe et al., 2017) were compared to predicted proteins encoded by the *N. benthamiana* genome. Sequences with >67% identity were selected as potential ASAT1 and ASAT2 candidates and nucleotide sequences were obtained from the Solanaceae Genomics Network (www.solgenomics.net). The candidate *ASAT* sequences were subsequently confirmed by comparison to the most recent published *N. benthamiana* genome assembly (Schiavinato et al., 2019). To

verify the nucleotide sequences of *N. benthamiana ASAT1* and *ASAT2*, the genes were amplified with ASAT1F/ASAT1R and ASAT2F/ASAT2R primers (Table **S4**) from genomic DNA. Amplified fragments were cloned in pDONOR™207 (ThermoFisher Scientific, US) and were sequenced in their entirety using Sanger sequencing, which showed no differences to the published *N. benthamiana* genome.

Phylogenetic analysis of N. benthamiana *ASATs*

A protein phylogenetic tree of previously annotated Solanaceae ASATs (Fig. **2, S1, S2**; Tables **S1, S2**) was constructed using maximum likelihood method. Briefly, the ASAT protein sequences were aligned in ClustalW (Thompson et al., 1994). Then the alignment was improved by removing the spurious sequences and poorly aligned regions (gap threshold at 0.25) using TrimAL v1.4 (Capella-Gutierrez et al., 2009). Finally, an unrooted maximum likelihood tree was generated using the improved alignment with a bootstrap of 1000 in RAxML v8.2.12 (Stamatakis, 2014). The tree was visualized and presented using FigTree v1.4.4 (http://tree.bio.ed.ac.uk).

sgRNA design and plasmid cloning

Single-guide RNAs (sgRNA) targeting *ASAT1* and *ASAT2* were designed based on the coding regions using CRISPR-P v2.0 (Liu et al., 2017) and CRISPRdirect (https://crispr.dbcls.jp/), based on cleavage efficiency and lack of potential off-target sites in the *N. benthamiana* genome. Additionally, only sgRNAs with >40% GC content were selected.

Three Cas9/gRNA constructs each were constructed for *ASAT1* and *ASAT2* following a previously developed CRISPR/Cas9 system (Jacobs et al., 2015). Four segments of DNA were prepared with 20-bp overlaps on their ends. 1) ssDNA gRNA oligonucleotides targeting either the sense or antisense sequence of target genes were designed as: sense oligo TCAAGCGAACCAGTAGGCTT-GN19-GTTTTAGAGCTAGAAATAGC, and antisense oligo GCTATTTCTAGCTCTAAAAC-N19C-AAGCCTACTGGTTCGCTTGA (the gRNA sequences are shown in Fig. **3**; Table **S4**), and synthesized by Integrated DNA Technologies (www.idtdna.com). One µl of each 100 µM oligo was added to 500 µl 1x NEB buffer 2 (New England Biolabs, www.neb.com). 2) The p201N:Cas9 plasmid was linearized by digestion with *Spe*1 (www.neb.com) in 1x buffer 4 at 37°C for 2 h, followed by column purification and a second digestion with *Swa*l in 1x buffer 3.1 at 25°C for 2 h. Complete plasmid digestion was confirmed on a 0.8% agarose gel. 3) The MtU6 promoter and 4) Scaffold DNAs were PCR-amplified from the pUC gRNA Shuttle plasmid (Jacobs et al., 2015) using the primers *Swa*l_MtU6F/MtU6R and ScaffoldF/Spe_ScaffoldR, respectively (Table **S4**). The PCR reactions were performed with a high-fidelity polymerase (2xKapa master mix; www.sigmaaldrich.com) using the program: 95°C for 3 min followed by 31 cycles of 98°C for 20 sec, 60°C for 30 sec, 72°C for 30 sec, and a final extension of 72°C

for 5 min. Finally, cloning was done using the NEBuilder® HiFi DNA Assembly Cloning Kit. For each reaction, the four pieces of DNA were mixed in a 20-µl reaction with the NEBbuilder assembly mix with a final concentration of 0.011 pmol (~100 ng) of p201N:Cas9 plasmid, 0.2 pmol of MtU6 amplicon (~50 ng), scaffold amplicon (~12 ng) and ssDNA gRNA oligo (60-mer, 1 µl). The reactions were incubated at 50°C for 1 h.

Two µl of the cloning reaction were transformed into 50 µl of One Shot™ Top10 chemically competent cells (Invitrogen, www.thermofisher.com) and plated on LB (Bertani, 1951) agar medium with 50 µl/ml kanamycin for transformant selection. Colonies with the correct inserts were screened using the Ubi3p218R and IScelR primers and confirmed by Sanger sequencing (Table **S4**). Plasmids carrying the designed gRNA constructs were transformed into *Agrobacterium tumefaciens* strain GV3101 for generating transgenic plants.

To avoid off-target effects, gRNAs were further checked by comparison against the reference *N. benthamiana* genome v1.0.1 (www.solgenomics.net). Only two sites were found to have non-target matches >17 nt (both with 1 internal mismatch), and with the NGG PAM sequence on the correct strand. These two sites were checked by PCR amplification and Sanger sequencing (primers in Table **S4**) and showed no unexpected editing in our *ASAT* mutant plants.

Stable mutagenesis of ASATs using tissue culture

Stable *ASAT* mutant *N. benthamiana* plants were created in the Boyce Thompson Institute plant transformation facility using CRISPR/Cas9 with gRNAs that had been confirmed to be functional in transient assays (Fig. **S9**) following a previously described protocol (Van Eck et al., 2019), with minor modifications.

Confirmation of homozygous mutant plants in the T2 generation

Rooted *N. benthamiana* plants from tissue culture were transferred to soil (T0 generation). CRISPR/Cas9-induced mutations were identified by PCR amplification of genomic regions of the gRNA target sites in *ASAT1* and *ASAT2* (Fig. **3**), followed by Sanger sequencing (primers in Table **S4**). Lines with mutations were used to generate T1 plants, which were subjected to PCR amplification and sequencing to confirm homozygous mutations. T2 seeds from confirmed homozygous mutant *asat1-1*, *asat1-2*, *asat2-1*, and *asat2-2* T1 plants were used for all experiments. Homozygous mutations were confirmed in randomly selected T2 plants by PCR amplification and Sanger sequencing. The presence or absence of Cas9 in transgenic plants in the T0, T1, and T2 generations was confirmed by PCR amplification (primers in Table **S4**) and agarose gel electrophoresis.

Acylsugar measurements by LC/MS

Liquid chromatography/mass spectrometry (LC/MS) was used to measure acylsugar content in leaf extracts from wildtype and *ASAT* mutant plants. New leaflets were rinsed in acylsugar extraction solution (3:3:2 acetonitrile:isopropanol:water, 0.1% formic acid, and 1 μM Telmisartan as internal standard) and gently agitated for 2 min. Then, the extraction solutions were transferred to LC/MS glass vials, and the leaves were air dried for leaf weight measurements.

Chromatography of leaf surface washes was performed on a ThermoScientific Ultimate 3000 HPLC with a glass vial autosampler coupled with a Thermo Scientific Q Exactive™ Hybrid Quadrupole-Orbitrap™ Mass Spectrometer at Boyce Thompson Institute. Acylsugar extracts were separated on an Ascentis Express C18 HPLC column (10 cm × 2.1 mm × 2.7 μm) (Sigma-Aldrich, St. Louis, MO) with a flow rate of 0.3 ml/min, using a gradient flow of 0.1% formic acid (Solvent A) and 100% acetonitrile (Solvent B). We used a 7-min LC method for metabolite profiling, which involved a linear gradient from 95:5 A:B to 0:98 A:B. Full-scan mass spectra were collected (mass range: m/z 50–1000) in both positive and negative electron spray ionization (ESI) modes. Mass spectral parameters were set as follows: capillary spray voltage 2.00 kV for negative ion-mode and 3.00 kV for positive ion-mode, source temperature: 100°C, desolvation temperature 350°C, desolvation nitrogen gas flow rate: 600 liters/h, cone voltage 35 V. Acylsugars were identified and annotated using Thermo Xcalibur Qual Browser (Thermo Fisher) and MS-DIAL v4.20 based on the MS/MS peak features and neutral losses (Fig. **S3**). The acylsugar abundances were estimated using peak areas at the respective *m/z* channel under negative ESI mode. Acylsugar quantification was first normalized to the internal control Telmisartan to account for technical variation, and then normalized to the leaf dry weight to allow comparisons between samples.

Insect choice and no-choice bioassays

To measure *M. persicae* and *M. euphorbiae* growth, we caged aphids on individual leaves of mutant and wildtype 4~5-week-old *N. benthamiana* (Fig. **S10a,b**). Twenty adult *M. persicae* from *N. tabacum* (naïve to *N. benthamiana*) were placed in each cage and allowed to generate nymphs for ~12 hrs. Twenty-five nymphs were left in each cage and were monitored for 5 d to assess nymph survival. At the end of the survival monitoring period, five *M. persicae* were left in each cage and reproduction was monitored for one week. The remaining *M. persicae* were collected to measure aphid size by imaging and assessing the area of each aphid using ImageJ (Schneider et al., 2012). Ten adult *M. euphorbiae* from a colony on tomato cv. Moneymaker were placed in each individual cage on *N. benthamiana* leaves. Surviving aphids and progeny were counted after 24 h.

M. persicae and *M. euphorbiae* choice assays were performed with detached leaves from 4~5-week-old *N. benthamiana*. Two similarly-sized leaves from individual *ASAT* mutant and wildtype plants

were cut and placed in 15-cm Petri dishes, with their petioles inserted in moistened cotton swabs (Fig. **S10c**). Ten naïve adult aphids were released at the midpoint between pairs of leaves (wildtype, *asat1*, or *asat2*), and the Petri dishes were placed under 16:8 h light:dark photoperiod. The aphids on each leaf were counted at 24 h after their release in the Petri dishes.

To measure whitefly survival and fecundity on wildtype and *asat2-1 N. benthamiana* plants, cages were set up with plants at the seven-leaf stage (~3 weeks old). Each cage contained three plants, either wildtype or *asat2-1*. Ninety adult whiteflies reared on *Brassica oleracea* (variety Earliana; www.burpee.com, catalog# 62729A) were introduced into each cage (60 x 60 x 60 cm) with *N. benthamiana* (30 whiteflies/plant) and were allowed to feed for three days at 26°C with a 16:8 h light:dark photoperiod. The numbers of whiteflies surviving on each host plant were counted, after which the remaining insects were killed with insecticidal soap. The following day, the number of whitefly eggs on each plant was counted. This experiment was conducted twice with similar results.

For whitefly choice assays, wildtype and *asat2-1* plants at the seven-leaf stage were placed together in the same cage. Approximately 150 whiteflies from cabbage plants were moved into each cage. After 24 h at 26°C with a 16:8 h light:dark photoperiod, live and dead whiteflies were counted on the plants and elsewhere in the cage. This experiment was repeated three times.

Eggs of *H. zea, H. virescens* and *T. ni* were hatched on artificial diet (Southland Products, Lake Village, Arkansas). Neonate larvae were confined onto individual *N. benthamiana* leaves, one larva/plant, using 10 x 15 cm organza mesh bags (www.amazon.com, item B073J4RS9C). After ten days, the surviving larvae were counted and weighed. In a separate experiment, *H. zea, H. virescens*, and *T. ni* were reared on artificial diet (beet armyworm diet, www.southlandproducts.net) for five days. Individual five-day-old caterpillars were weighed and then confined on 4~4.5-week-old *N benthamiana* plants using 30 cm x 60 cm micro-perforated bread bags (www.amazon.com). After seven days, the surviving larvae were weighed again. Relative growth rate was calculated as: ln(((day-12 mass)/(mean day-5 mass))/7).

Leaf water loss and temperature assays

To measure the leaf water loss, two leaves from each of eight plants were detached. The fresh weight of each leaf was determined on a Sartorius Ultra Micro Balance. All leaves were placed at 23°C and a 16:8 h light:dark photoperiod. Each leaf was weighted again after 24 h and the percentage of water loss was calculated as [(fresh_weight – final_weight)/fresh_weight]*100%.

Thermal images were acquired in the growth chamber using a thermal camera (A655sc, FLIR Systems Inc., Boston, MA) with a spectral range of 7.5–14.0 mm and a resolution of 640 x 480 pixels. The camera was placed ~1 m away from each plant and a white background was used when the plant images were acquired. One region of interest (ROI), corresponding to the perimeter of each leaf, was

specified per leaf for 20 leaves per genotype. Using the FLIR ResearchIR Max software v.4.40.9.30, thermal images files were exported as CSV files. Images were segmented from the background using Gaussian mixture models in MATLAB to determine the temperature of each leaf. After segmentation, the temperature was averaged across the segmented leaf.

Hyperspectral images were acquired in a dark room using a hyperspectral imager (SOC710, Series 70-V, Surface Optics Corporation, San Diego, CA) that covered a 400-1000 nm spectral range for 128 wavebands. Image acquisition were performed using a Dell DELL XPS 15 9570 laptop computer that controls the camera. The camera was fixed ~1 m above the plants and capturing top view images. A Spectralon tile (Labsphere Inc, North Sutton, NH) was placed next to the plant trays, covering one corner of the image to facilitate subsequent image processing and calibration. The nominal reflectance value for the Spectralon tile was 99% with a 30.5x30.5 cm^2 reflective area. Lighting consisted of two halogen lamps placed at ~45° angles on either side of the camera to create an even light distribution. All image analysis was performed in HSIviewer, a MATLAB package (Stone et al., 2020). White reflectance calibration was performed using the Spectralon tile. One ROI was specified for each of 20 leaves per genotype. This ROI corresponded to the perimeter of each leaf. From each hyperspectral cube image, the vegetation pixels (green portion of the plant) were extracted using the Normalized Difference Vegetation Index (NDVI). Mean reflectance (R) was calculated per band per 10 leaves in order to obtain the water band index (WBI) results. To calculate NDVI and WBI we used the following formulas, where *R* corresponds to the reflectance at a specific wavelength (nm): WBI = (R970/R900) (Penuelas et al., 1993) and NVDI = (R750 - R705)/(R750 + R705) (Gitelson and Merzlyak, 1994).

Statistical analysis

All statistical comparisons were conducted using SPSS v25, R and MATLAB R2019a (MathWorks, Inc., Natick, MA, USA). ANOVA followed by a Dunnett's post hoc test was used to determine differences in leaf water loss, leaf temperature, and WBI across genotypes in each data set. ANOVA followed by a Duncan post hoc test was used for aphid bioassay and LC/MS results. A Chi-square test was used to test for differences in pairwise aphid choice assays, whitefly, and lepidopteran assays. Raw data for all figures are shown in Table S3.

Declarations:

Acknowledgements

We thank Patricia Keen and Joyce Van Eck for their help with *N. benthamiana* stable transformation, Ning Zhang and Greg Martin for sharing the p201N-Cas9 construct and the *Drm3* sgRNA control constructs, and William Stone and Thomas Lawton for providing custom image processing software.

Funding

This research was supported by Cornell startup funds to G.D.M., Deutsche Forschungsgemeinschaft award #411255989 to L.H.K., and United States Department of Agriculture Biotechnology Risk Assessment Grant 2017-33522-27006, US National Science Foundation award IOS-1645256, and Defense Advanced Research Projects Agency (DARPA) agreement HR0011-17-2-0053 to G.J, and US National Science Foundation award #1723926 to C.L.C. G.S. is part of a team supporting DARPA's Insect Allies program under agreement HR0011-17-2-0055. M.A.G. is part of a team supporting DARPA's Advanced Plant Technologies program under agreement HR0011-18-C-0146. The views and conclusions contained in this document are those of the authors and should not be interpreted as representing the official policies of the U.S. Government.

Conflict of interest

The authors declare that there is no conflict of interest.

Availability of data and material

All data generated or analyzed during this study are included in this published article and its supplementary information files.

Code availability

Not applicable

Authors' Contributions

G.J. and H.F. conceived the original research plans; H.F., S.S., L.A., H.X., L.K., J.D.T, S.H.C., and A.N.F. performed the experiments; H.F., L.A., L.K., and G.D.M. analyzed the data; C.L.C., M.A.G., G.D.M., G.S., and G.J. supervised the experiments; H.F. and G.J. wrote the article with contributions from all of the authors; G.J. agrees to serve as the contact author responsible for communication and distribution of samples.

Ethics approval

Not applicable

Consent to Participate

Not applicable

Consent for publication

Not applicable

References

Arntzen C (2015) Plant-made pharmaceuticals: from 'Edible Vaccines' to Ebola therapeutics. Plant Biotechnology Journal 13: 1013-1016

Arrendale RF, Severson RF, Sisson VA, Costello CE, Leary JA, Himmelsbach DS, Vanhalbeek H (1990) Characterization of the sucrose ester fraction from *Nicotiana glutinosa*. Journal of Agricultural and Food Chemistry 38: 75-85

Bally J, Jung H, Mortimer C, Naim F, Philips JG, Hellens R, Bombarely A, Goodin MM, Waterhouse PM (2018) The rise and rise of *Nicotiana benthamiana*: a plant for all reasons. Annual Review of Phytopathology, Vol 56 56: 405-426

Bertani G (1951) Studies on lysogenesis. I. The mode of phage liberation by lysogenic *Escherichia coli*. J Bacteriol 62: 293-300

Bombarely A, Rosli HG, Vrebalov J, Moffett P, Mueller LA, Martin GB (2012) A draft genome sequence of *Nicotiana benthamiana* to enhance molecular plant-microbe biology research. Mol Plant-Micr Int 25: 1523-1530

Bos JI, Prince D, Pitino M, Maffei ME, Win J, Hogenhout SA (2010) A functional genomics approach identifies candidate effectors from the aphid species Myzus persicae (green peach aphid). PLoS Genet 6: e1001216

Capella-Gutierrez S, Silla-Martinez JM, Gabaldon T (2009) trimAl: a tool for automated alignment trimming in large-scale phylogenetic analyses. Bioinformatics 25: 1972-1973

Cardoso MZ (2008) Herbivore handling of a plant's trichome: The case of *Heliconius charithonia* (L.) (Lepidoptera : Nymphalidae) and *Passiflora Lobata* (Killip) Hutch. (Passifloraceae). Neotropical Entomology 37: 247-252

Casteel CL, Yang C, Nanduri AC, De Jong HN, Whitham SA, Jander G (2014) The NIa-Pro protein of turnip mosaic virus improves growth and reproduction of the aphid vector, *Myzus persicae* (green peach aphid). Plant J 77: 653-663

Chortyk OT, Pomonis JG, Johnson AW (1996) Syntheses and characterizations of insecticidal sucrose esters. J Ag Food Chem 44: 1551-1557

Clay N, Adio A, Denoux C, Jander G, Ausubel F (2009) Glucosinolate metabolites required for an Arabidopsis innate immune response. Science 323: 95-101

D'Auria JC (2006) Acyltransferases in plants: a good time to be BAHD. Curr Opin Plant Biol 9: 331-340

Egan AN, Moore S, Stellari GM, Kang BC, Jahn MM (2019) Tandem gene duplication and recombination at the AT3 locus in the *Solanaceae*, a gene essential for capsaicinoid biosynthesis in *Capsicum*. Plos One 14: e0210510

Egea I, Albaladejo I, Meco V, Morales B, Sevilla A, Bolarin MC, Flores FB (2018) The drought-tolerant *Solanum pennellii* regulates leaf water loss and induces genes involved in amino acid and ethylene/jasmonate metabolism under dehydration. Sci Rep 8: 2791

Ellison EE, Nagalakshmi U, Gamo ME, Huang PJ, Dinesh-Kumar S, Voytas DF (2020) Multiplexed heritable gene editing using RNA viruses and mobile single guide RNAs. Nat Plants 6: 620-624

Elzinga DA, De Vos M, Jander G (2014) Suppression of plant defenses by a *Myzus persicae* (green peach aphid) salivary effector protein. Mol Plant Microbe Interact 27: 747-756

Fan P, Miller AM, Schilmiller AL, Liu X, Ofner I, Jones AD, Zamir D, Last RL (2016) In vitro reconstruction and analysis of evolutionary variation of the tomato acylsucrose metabolic network. Proc Natl Acad Sci U S A 113: E239-248

615 Feng H, Jander G (2021) Rapid screening of *Myzus persicae* (green peach aphid) RNAi targets using
616 *Tobacco rattle virus*. Methods Mol Biol in press
617 Fobes JF, Mudd JB, Marsden MP (1985) Epicuticular lipid accumulation on the leaves of *Lycopersicon*
618 *pennellii* (Corr.) D'Arcy and *Lycopersicon esculentum* Mill. Plant Physiol 77: 567-570
619 Gaquerel E, Kotkar H, Onkokesung N, Galis I, Baldwin IT (2013) Silencing an N-acyltransferase-like
620 involved in lignin biosynthesis in *Nicotiana attenuata* dramatically alters herbivory-induced
621 phenolamide metabolism. Plos One 8: e62336
622 Gitelson A, Merzlyak MN (1994) Spectral reflectance changes associated with autumn senescence of
623 *Aesculus hippocastanum* L and *Acer platanoides* L leaves - spectral features and relation to
624 chlorophyll estimation. J Plant Physiol 143: 286-292
625 Glas JJ, Schimmel BCJ, Alba JM, Escobar-Bravo R, Schuurink RC, Kant MR (2012) Plant glandular
626 trichomes as targets for breeding or engineering of resistance to herbivores. International Journal
627 of Molecular Sciences 13: 17077-17103
628 Gong P, Zhang J, Li H, Yang C, Zhang C, Zhang X, Khurram Z, Zhang Y, Wang T, Fei Z, Ye Z (2010)
629 Transcriptional profiles of drought-responsive genes in modulating transcription signal
630 transduction, and biochemical pathways in tomato. J Exp Bot 61: 3563-3575
631 Goodin MM, Zaitlin D, Naidu RA, Lommel SA (2008) *Nicotiana benthamiana*: its history and future as a
632 model for plant-pathogen interactions. Mol Plant Microbe Interact 21: 1015-1026
633 Hagimori M, Matsui M, Matsuzaki T, Shinozaki Y, Shinoda T, Harada H (1993) Production of somatic
634 hybrids between *Nicotiana benthamiana* and *Nicotiana tabacum* and their resistance to aphids.
635 Plant Science 91: 213-222
636 Jacobs TB, LaFayette PR, Schmitz RJ, Parrott WA (2015) Targeted genome modifications in soybean
637 with CRISPR/Cas9. Bmc Biotechnology 15: 16
638 Karabourniotis G, Kotsabassidis D, Manetas Y (1995) Trichome density and its protective potential
639 against ultraviolet-B radiation damage during leaf development. Canadian Journal of Botany-
640 Revue Canadienne De Botanique 73: 376-383
641 Kim J, Kang K, Gonzales-Vigil E, Shi F, Jones AD, Barry CS, Last RL (2012) Striking natural diversity
642 in glandular trichome acylsugar composition is shaped by variation at the acyltransferase2 locus
643 in the wild tomato *Solanum habrochaites*. Plant Physiol 160: 1854-1870
644 Kroumova AB, Wagner GJ (2003) Different elongation pathways in the biosynthesis of acyl groups of
645 trichome exudate sugar esters from various solanaceous plants. Planta 216: 1013-1021
646 Kroumova ABM, Zaitlin D, Wagner GJ (2016) Natural variability in acyl moieties of sugar esters
647 produced by certain tobacco and other *Solanaceae* species. Phytochemistry 130: 218-227
648 Laue G, Preston CA, Baldwin IT (2000) Fast track to the trichome: induction of N-acyl nornicotines
649 precedes nicotine induction in *Nicotiana repanda*. Planta 210: 510-514
650 Leong BJ, Lybrand DB, Lou YR, Fan PX, Schilmiller AL, Last RL (2019) Evolution of metabolic
651 novelty: A trichome-expressed invertase creates specialized metabolic diversity in wild tomato.
652 Science Advances 5: eaaw3754
653 Liu H, Ding YD, Zhou YQ, Jin WQ, Xie KB, Chen LL (2017) CRISPR-P 2.0: an improved CRISPR-
654 Cas9 tool for genome editing in plants. Molecular Plant 10: 530-532
655 Marchant WG, Legarrea S, Smeda JR, Mutschler MA, Srinivasan R (2020) Evaluating acylsugars-
656 mediated resistance in tomato against *Bemisia tabaci* and transmission of tomato yyellow leaf
657 curl virus. Insects 11: 842
658 Matsuzaki T, Shinozaki Y, Hagimori M, Tobita T, Shigematsu H, Koiwai A (1992) Novel glycerolipids
659 and glycolipids from the surface-lipids of *Nicotiana benthamiana*. Bioscience Biotechnology and
660 Biochemistry 56: 1565-1569
661 Matsuzaki T, Shinozaki Y, Suhara S, Ninomiya M, Shigematsu H, Koiwai A (1989) Isolation of
662 glycolipids from the surface-lipids of *Nicotiana bigelovii* and their distribution in *Nicotiana*
663 species. Agricultural and Biological Chemistry 53: 3079-3082
664 McKenzie CL, Puterka GJ (2004) Effect of sucrose octanoate on survival of nymphal and adult
665 *Diaphorina citri* (Homoptera : Psyllidae). J Econ Entomol 97: 970-975

McKenzie CL, Weathersbee AA, 3rd, Puterka GJ (2005) Toxicity of sucrose octanoate to egg, nymphal, and adult *Bemisia tabaci* (Hemiptera: Aleyrodidae) using a novel plant-based bioassay. J Econ Entomol 98: 1242-1247

Meihls LN, Handrick V, Glauser G, Barbier H, Kaur H, Haribal MM, Lipka AE, Gershenzon J, Buckler ES, Erb M, Köllner TG, Jander G (2013) Natural variation in maize aphid resistance is associated with 2,4-dihydroxy-7-methoxy-1,4-benzoxazin-3-one glucoside methyltransferase activity. Plant Cell 25: 2341-2355

Moghe GD, Leong BJ, Hurney SM, Jones AD, Last RL (2017) Evolutionary routes to biochemical innovation revealed by integrative analysis of a plant-defense related specialized metabolic pathway. Elife 6: e28468

Ning J, Moghe GD, Leong B, Kim J, Ofner I, Wang Z, Adams C, Jones AD, Zamir D, Last RL (2015) A feedback-insensitive isopropylmalate synthase affects acylsugar composition in cultivated and wild tomato. Plant Physiol 169: 1821-1835

O' Connell MA, Medina AL, Sanchez Pena Pand Trevino MB (2007) Molecular genetics of drought resistance response in tomato and related species. In Razdan, M. K., & Mattoo, A. K. (eds). Genetic Improvement of Solanaceous Crops 2: Enfield USA 261-283

Penuelas J, Filella I, Biel C, Serrano L, Save R (1993) The reflectance at the 950-970 nm region as an indicator of plant water status. International Journal of Remote Sensing 14: 1887-1905

Powell JD (2015) From pandemic preparedness to biofuel production: tobacco finds its biotechnology niche in North America. Agriculture-Basel 5: 901-917

Ramsey JS, Elzinga DA, Sarkar P, Xin YR, Ghanim M, Jander G (2014) Adaptation to nicotine feeding in *Myzus persicae*. J Chem Ecol 40: 869-877

Ramsey JS, Wilson AC, De Vos M, Sun Q, Tamborindeguy C, Winfield A, Malloch G, Smith DM, Fenton B, Gray SM, Jander G (2007) Genomic resources for *Myzus persicae:* EST sequencing, SNP identification, and microarray design. BMC Genomics 8: 423

Rodriguez AE, Tingey WM, Mutschler MA (1993) Acylsugars of *Lycopersicon pennellii* deter settling and feeding of the green peach aphid (Homoptera, Aphididae). Journal of Economic Entomology 86: 34-39

Rodriguez PA, Stam R, Warbroek T, Bos JI (2014) Mp10 and Mp42 from the aphid species Myzus persicae trigger plant defenses in Nicotiana benthamiana through different activities. Mol Plant Microbe Interact 27: 30-39

Schiavinato M, Strasser R, Mach L, Dohm JC, Himmelbauer H (2019) Genome and transcriptome characterization of the glycoengineered *Nicotiana benthamiana* line DeltaXT/FT. BMC Genomics 20: 594

Schilmiller A, Shi F, Kim J, Charbonneau AL, Holmes D, Jones AD, Last RL (2010) Mass spectrometry screening reveals widespread diversity in trichome specialized metabolites of tomato chromosomal substitution lines. Plant Journal 62: 391-403

Schilmiller AL, Charbonneau AL, Last RL (2012) Identification of a BAHD acetyltransferase that produces protective acyl sugars in tomato trichomes. Proc Natl Acad Sci U S A 109: 16377-16382

Schilmiller AL, Moghe GD, Fan P, Ghosh B, Ning J, Jones AD, Last RL (2015) Functionally divergent alleles and duplicated Loci encoding an acyltransferase contribute to acylsugar metabolite diversity in *Solanum* trichomes. Plant Cell 27: 1002-1017

Schneider CA, Rasband WS, Eliceiri KW (2012) NIH Image to ImageJ: 25 years of image analysis. Nature Methods 9: 671-675

Shepherd RW, Wagner GJ (2007) Phylloplane proteins: emerging defenses at the aerial frontline? Trends in Plant Science 12: 51-56

Simmons AT, Gurr GM, McGrath D, Martin PM, Nicol HI (2004) Entrapment of *Helicoverpa armigera* (Hubner) (Lepidoptera:Noctuidae) on glandular trichomes of *Lycopersicon* species. Australian Journal of Entomology 43: 196-200

716 Simon B, Cenis JL, Demichelis S, Rapisarda C, Caciagli P, Bosco D (2003) Survey of *Bemisia tabaci*
717 (Hemiptera: Aleyrodidae) biotypes in Italy with the description of a new biotype (T) from
718 *Euphorbia characias*. Bull Entomol Res 93: 259-264
719 Slocombe SP, Schauvinhold I, McQuinn RP, Besser K, Welsby NA, Harper A, Aziz N, Li Y, Larson TR,
720 Giovannoni J, Dixon RA, Broun P (2008) Transcriptomic and reverse genetic analyses of
721 branched-chain fatty acid and acyl sugar production in *Solanum pennellii* and *Nicotiana*
722 *benthamiana*. Plant Physiol 148: 1830-1846
723 Song Z, Li S, Chen X, Liu L, Song Z (2006) Synthesis of sucrose esters. Forestry Studies in China 8: 26-
724 29
725 Stamatakis A (2014) RAxML version 8: a tool for phylogenetic analysis and post-analysis of large
726 phylogenies. Bioinformatics 30: 1312-1313
727 Stone WD, Pellicore MJ, Hagstrom S, Lawton TJ (2020) HSIviewer: Pushbutton hyperspectral image
728 analysis for rapid plant phenotyping. in review
729 Thompson JD, Higgins DG, Gibson TJ (1994) Clustal-W - Improving the sensitivity of progressive
730 multiple sequence alignment through sequence weighting, position-specific gap penalties and
731 weight matrix choice. Nucleic Acids Research 22: 4673-4680
732 Thurston R (1961) Resistance in *Nicotiana* to the green peach aphids and some other tobacco insect pest.
733 Journal of Economic Entomology 54: 946-949
734 Van Eck J, Keen P, Tjahjadi M (2019) *Agrobacterium tumefaciens*-mediated transformation of tomato.
735 Methods Mol Biol 1864: 225-234
736 Van T, Weinhold A, Ullah C, Dressel S, Schoettner M, Gase K, Gaquerel E, Xu SQ, Baldwin IT (2017)
737 O-acyl sugars protect a wild tobacco from both native fungal pathogens and a specialist
738 herbivore. Plant Physiology 174: 370-386
739 Wagner GJ, Wang E, Shepherd RW (2004) New approaches for studying and exploiting an old
740 protuberance, the plant trichome. Annals of Botany 93: 3-11
741 Weinhold A, Baldwin IT (2011) Trichome-derived O-acyl sugars are a first meal for caterpillars that tags
742 them for predation. Proceedings of the National Academy of Sciences of the United States of
743 America 108: 7855-7859
744

Figures

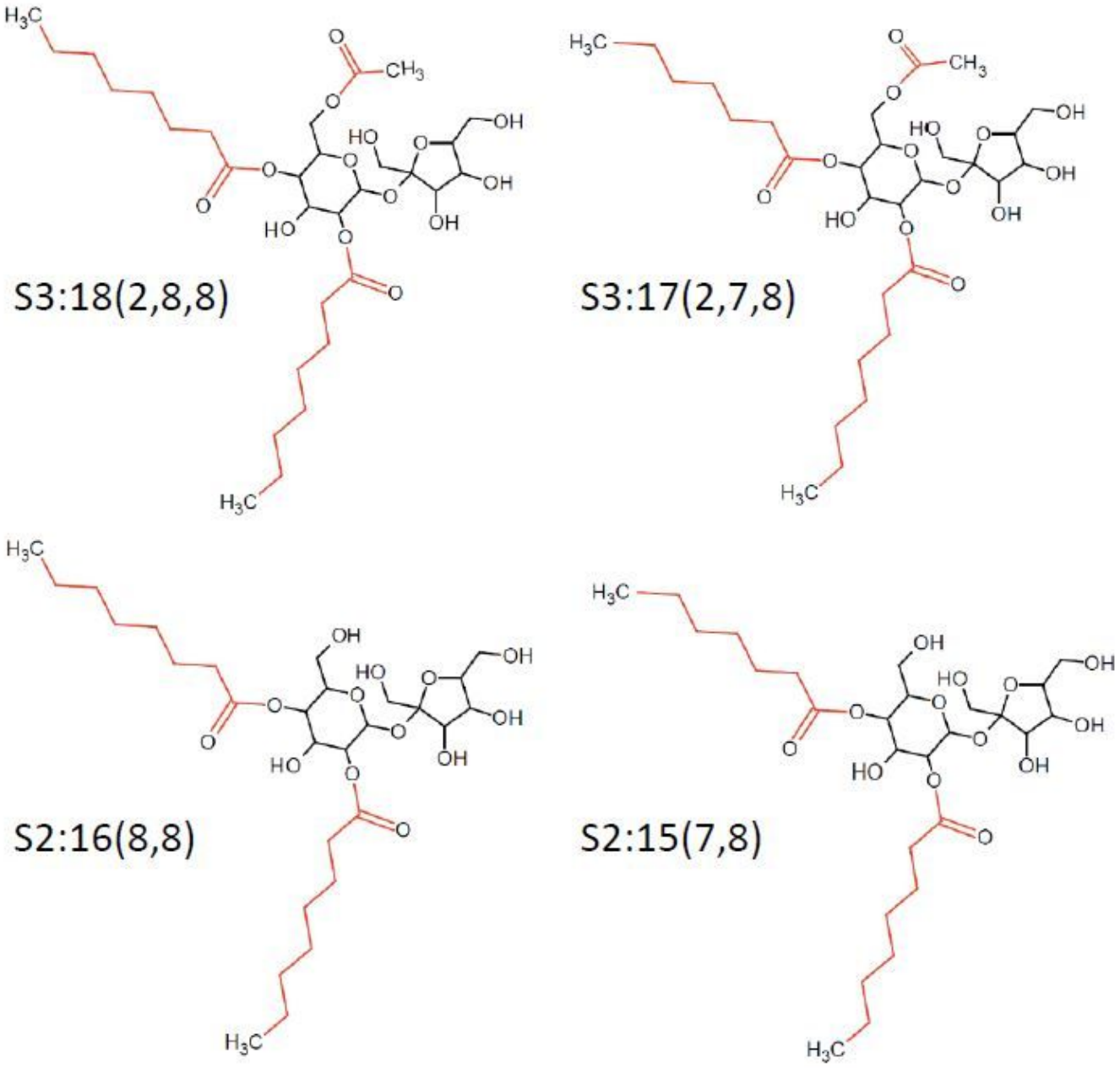

Figure 1

Predominant acylsugars in Nicotiana benthamiana Acylsucroses S3:17(2,7,8), S3:18(2,8,8), S2:16(8,8) and S2:15(7,8) are present in N. benthamiana. In the acylsugar structure names, S refers to sucrose, followed by the number of acyl chains, the total length of acyl chains, and the length of each individual chain in parentheses. Although the presence of C2, C7, and C8 chain lengths is confirmed, the specific positions of the acyl chains on the sucrose molecule are hypothesized based on previous observations of acylsugars in Nicotiana alata (Moghe et al, 2017), the predicted evolution of the acylsugar biosynthetic pathway, and enzyme promiscuities in the Solanaceae family.

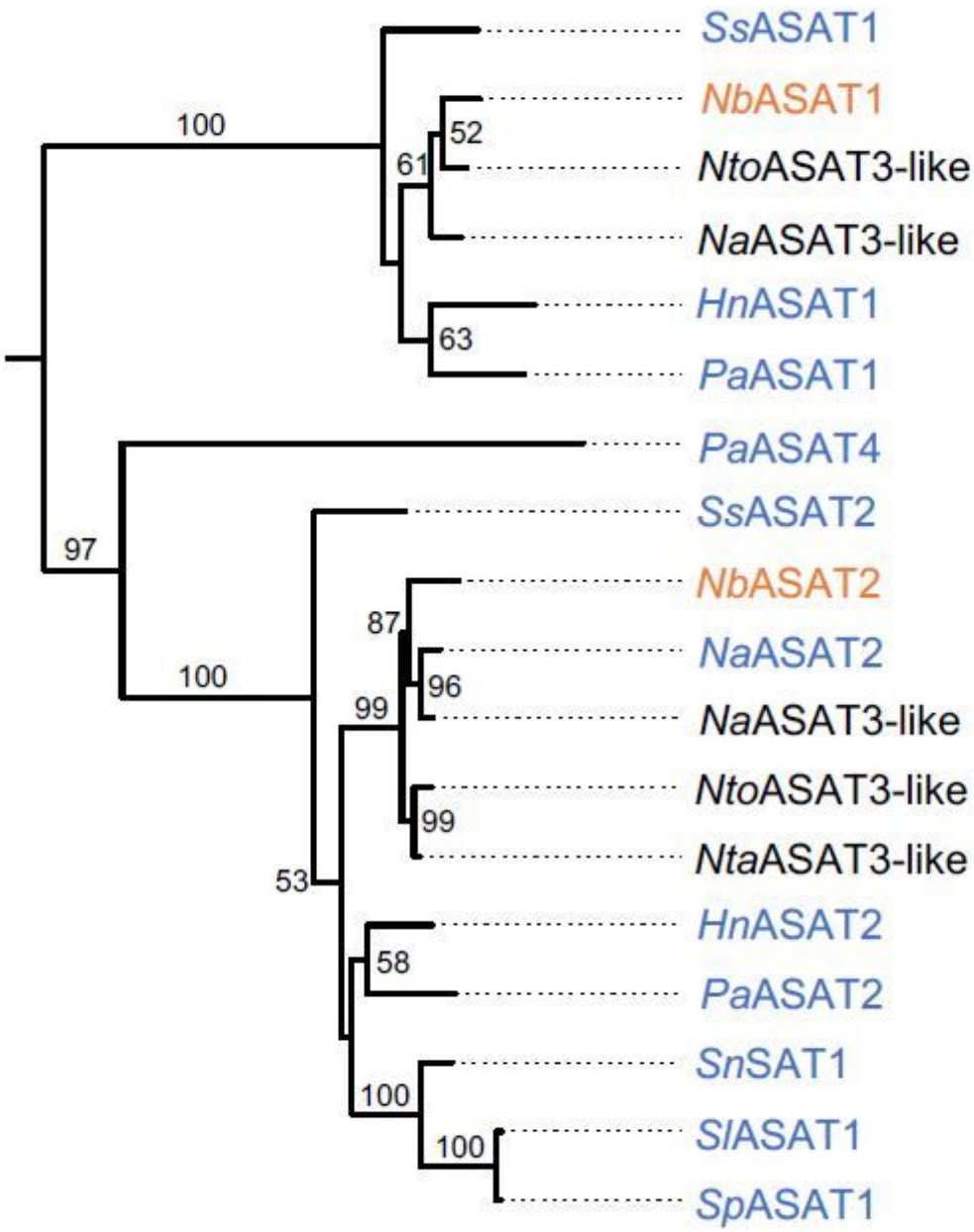

Figure 2

ASAT phylogenetic tree The evolutionary history of ASATs in the Solanaceae (Tables S1 and S2) was inferred using the Maximum Likelihood method in RAxML. Presented is a subtree of a larger tree that includes all annotated ASATs (Figure S1). The branch labels indicate the percentage of trees in which the associated taxa clustered together (bootstrap of 1000). Only values greater than 50 are presented. The two predicted N. benthamiana ASATs are highlighted in orange and ASATs that were previously chemically characterized are highlighted in blue. Ss = Salpiglossis sinuata, Nb = Nicotiana benthamiana, Nto = Nicotiana tomentosiformis, Na = Nicotiana attenuata, Hn = Hyoscyamus niger, Pa = Petunia

axillaris, Nta = Nicotiana tabacum, Sn = Solanum nigrum, Sl = Solanum lycopersicum, Sp = Solanum pennellii.

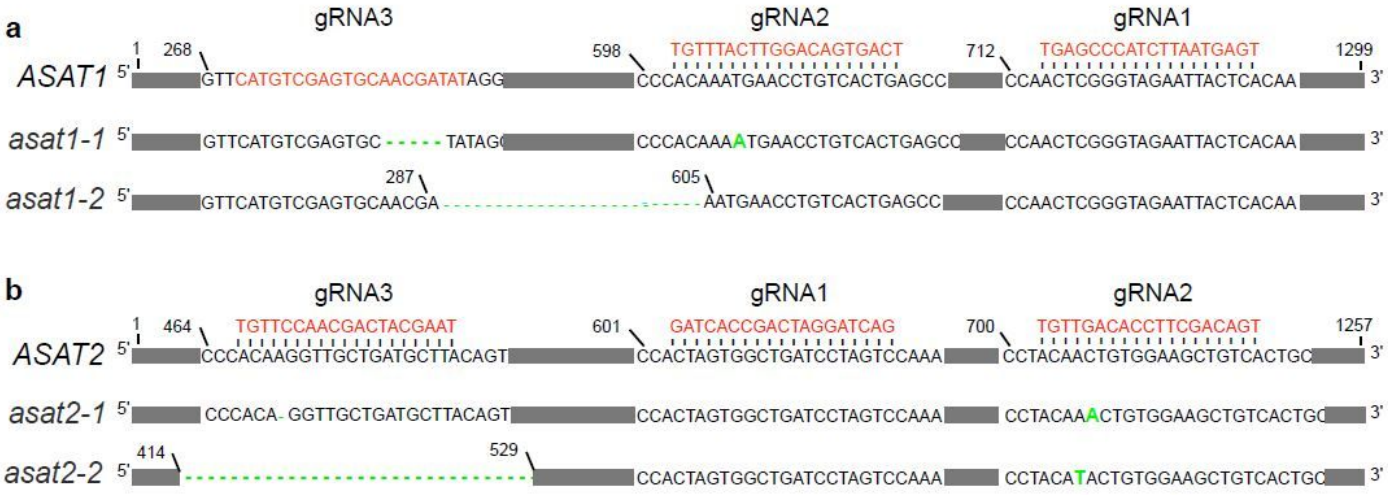

Figure 3

N. benthamiana ASAT mutations produced with CRISPR/Cas9 Three gRNAs (sequences shown in red) were designed to edit either ASAT1 or ASAT2. Whereas gRNA3 for ASAT1 is on the sense strand, the other gRNAs are on the antisense strand. For both ASAT1 and ASAT2, we obtained two independent mutations resulting from the corresponding gRNA2 and gRNA3. Single-base mutations and deletions are shown in green. (a) asat1-1 has a five-nucleotide deletion at gRNA3 and a single-nucleotide insertion at gRNA2. asat1-2 has a 318-nucleotide deletion between the gRNA3 and gRNA2 cutting sites. (b) asat2-1 has a single-nucleotide deletion at gRNA3 and single-nucleotide insertion at gRNA2 leading to a translation frame shift between the two mutations. asat2-2 has a 115-nucleotide deletion at gRNA3 and a single-nucleotide insertion leading to a translation frame shift at gRNA2.

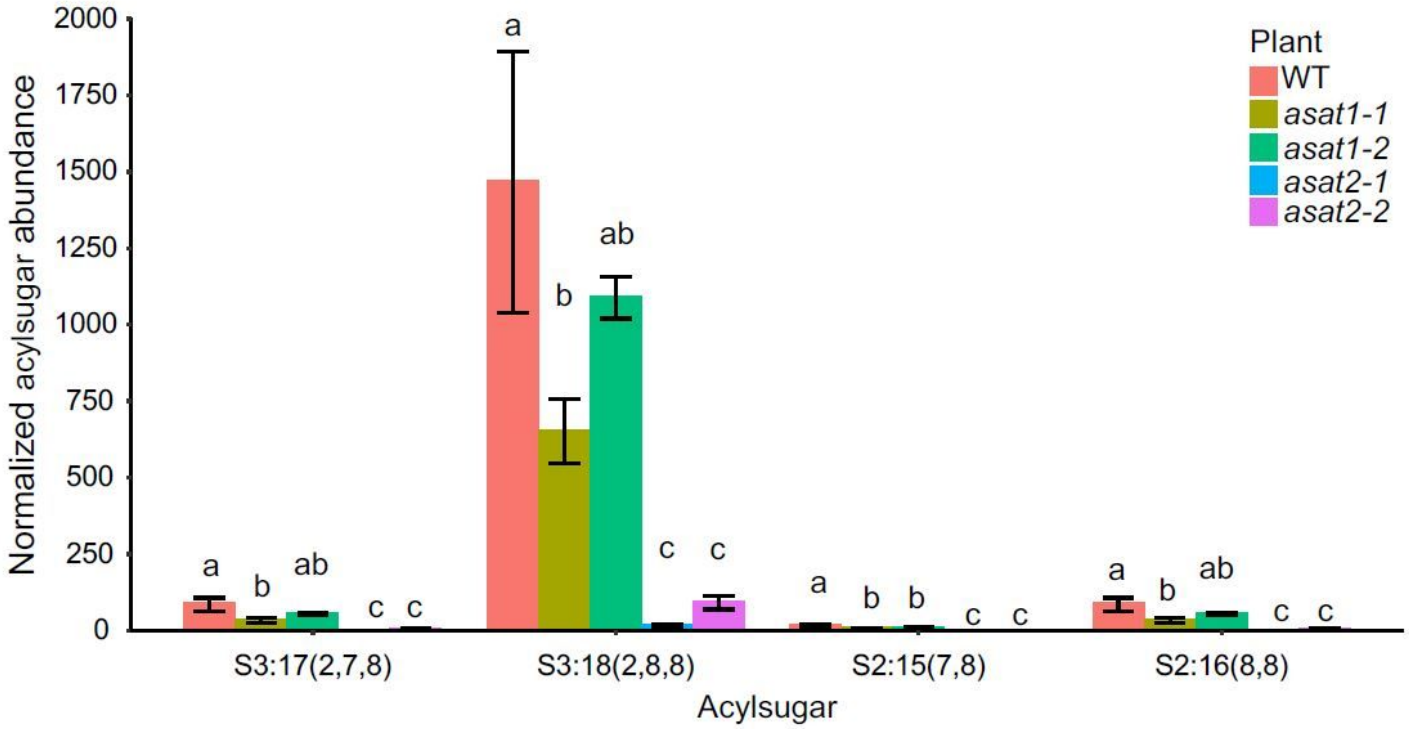

Figure 4

Abundance of two Nicotiana benthamiana acylsugars (S2:17(2,7,8) and S2:18(2,8,8)), and two likely pathway intermediates/fragmentations (S2:15(7,8) and S2:16(8,8)) Acyl sugar LC/MS peak areas were normalized relative to the peak area of Telmisartan, which was added as an internal control, and then to the leaf dry weight (per gram). Error bars represent standard errors from measurements of three plants of each genotype. Significant differences for each acylsugar between different genotypes were tested using one-way ANOVA followed by a Duncan's post hoc test ($p < 0.05$). Differences between groups are denoted with letters.

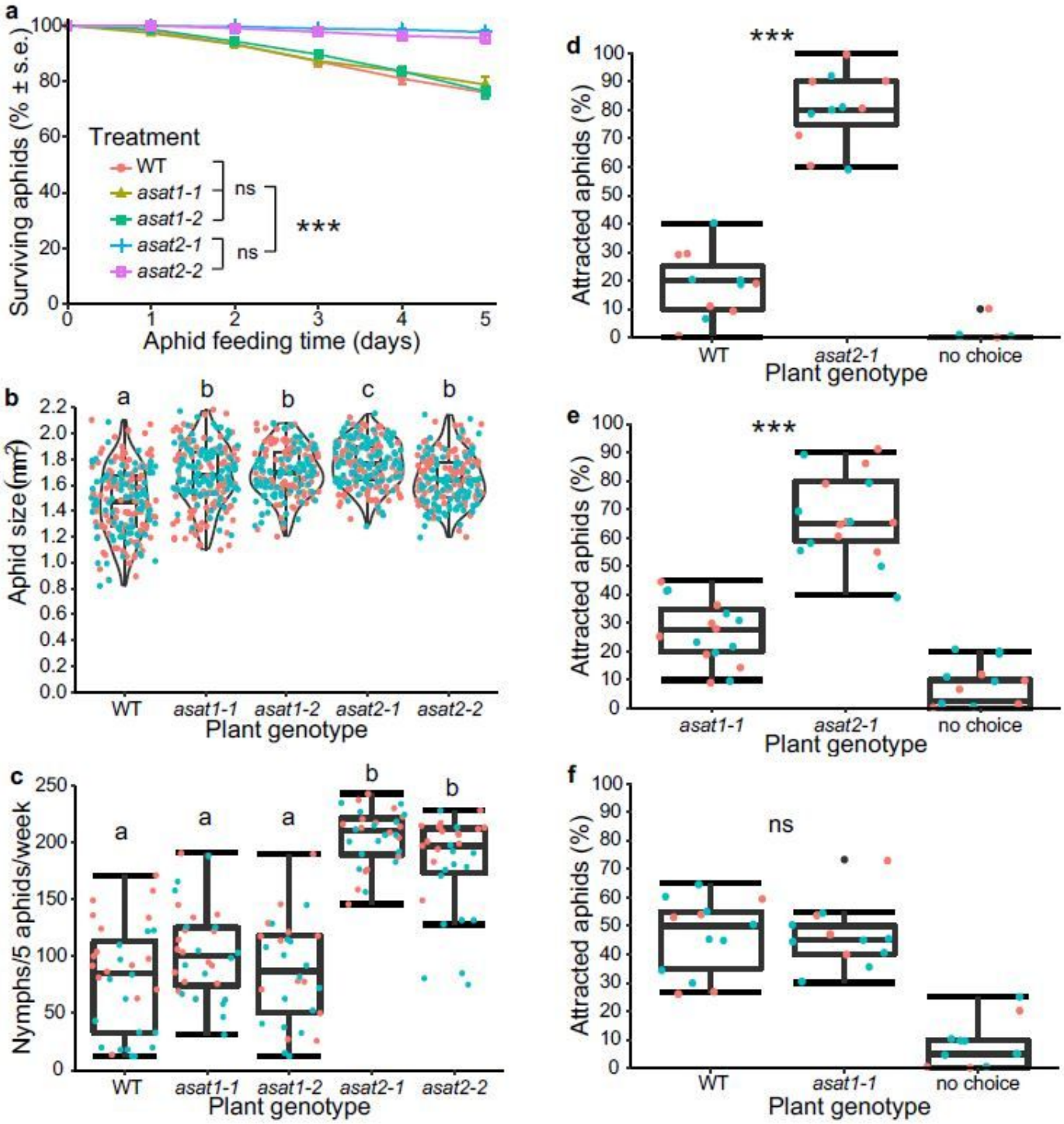

Figure 5

Myzus persicae bioassays with wildtype (WT), asat1, and asat2 Nicotiana benthamiana Data shown in all panels were combined from two independent experiments, which are shown in color orange and cyan in panels B-F. (a) Survival over 5 days of nymphs placed onto mutant and wildtype N. benthamiana. Significant differences are indicated for the 5-day time point: ns: not significant, *** $p < 0.001$, mean +/- s.e. of n = 15-16. Significant differences were tested using one-way ANOVA with a fixed factor of genotypes and a block effect of experiment followed by a Bonferroni post hoc test for multiple comparisons. Full statistical data for all time points are in Table S4. (b) Aphid growth, as measured by

body size after 5 days feeding on N. benthamiana. (c) Aphid reproduction, as measured by the number of nymphs that were produced by five aphids in one week. Significant differences between different groups ($p < 0.05$) were determined using ANOVA with a fixed factor of genotypes and a block effect of experiment followed by a Duncan's post hoc test and are indicated by lowercase letters above each group in panels B and C. (d-f) Aphid choice among detached leaves of each plant genotype, significant differences between genotypes were assessed using Chi-square tests, *** $p < 0.001$; ns: no significant difference; no choice: aphids were elsewhere in the Petri dish and not on a leaf. The box plots show the median, interquartile range, maximum and minimum after removal of outliers, and the individual data points.

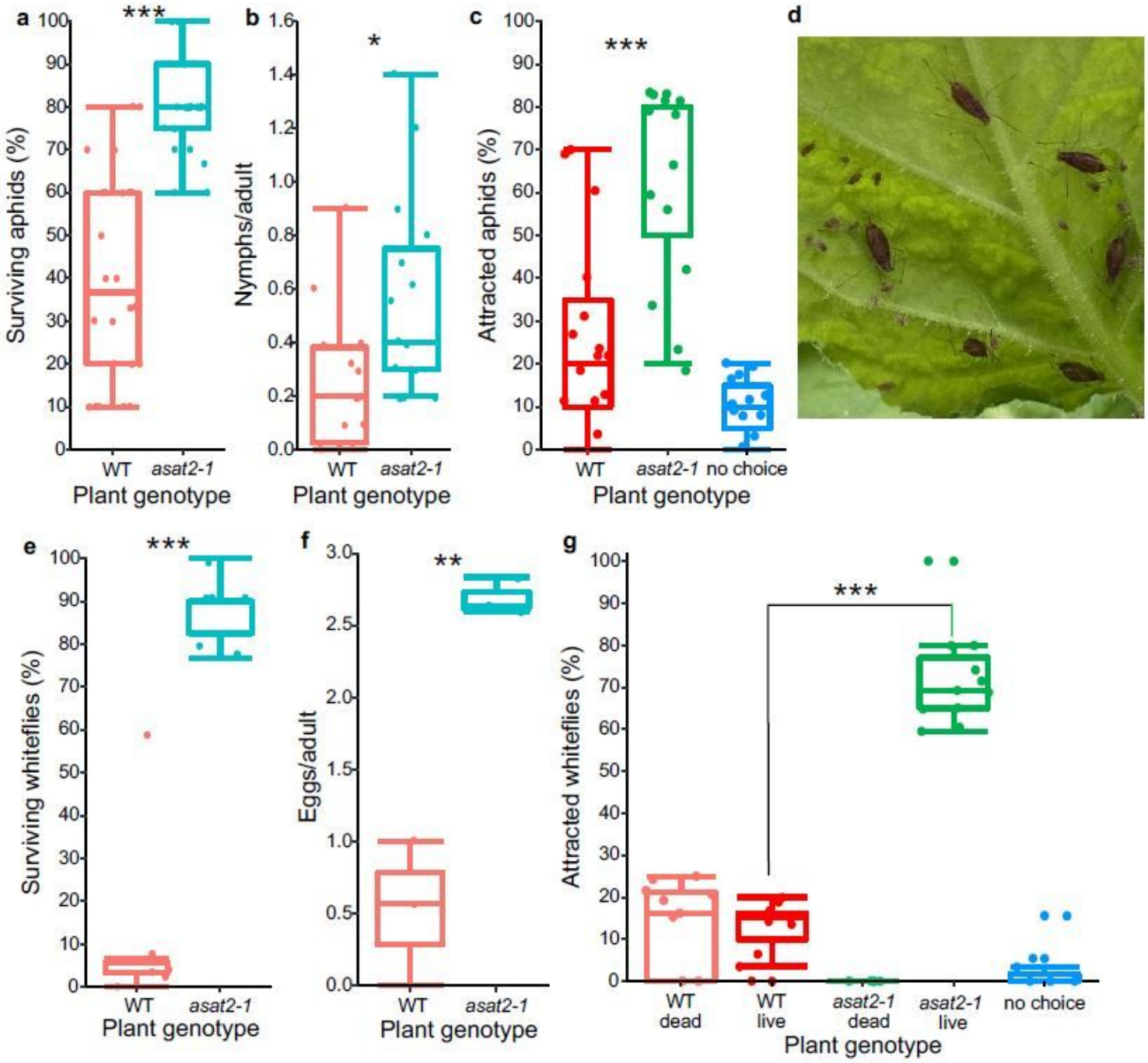

Figure 6

Potato aphid and whitefly bioassays on asat2-1 and wildtype (WT) N. benthamiana. (a-d) potato aphid (M. euphorbiae) bioassays. (a) aphid survival in 24 hours (n=15). (b) aphid reproduction in 24 hours (n=15). (c) aphid choices between detached leaves of each plant genotype (n=15). (d) An established M. euphorbiae colony on an N. benthamiana asat2-1 leaf. (e-g) whitefly bioassays. (e) whitefly survival in 3 days (n=6). (f) whitefly reproduction measured as number of eggs produced per adults in 3 days (n=3). (g) whitefly choices between plants of each genotype (n=3 for 4 independent experiments). Significantly differences were tested using independent t-tests for aphid and whitefly survival and reproduction data. Chi-square tests were used for aphid and whitefly choice assays. * $p < 0.05$, ** $p < 0.01$, *** $p < 0.001$; no choice: insects were not on a leaf at the end of the experiment. The box plots show the median, interquartile range, maximum and minimum after removal of outliers, and the individual data points.

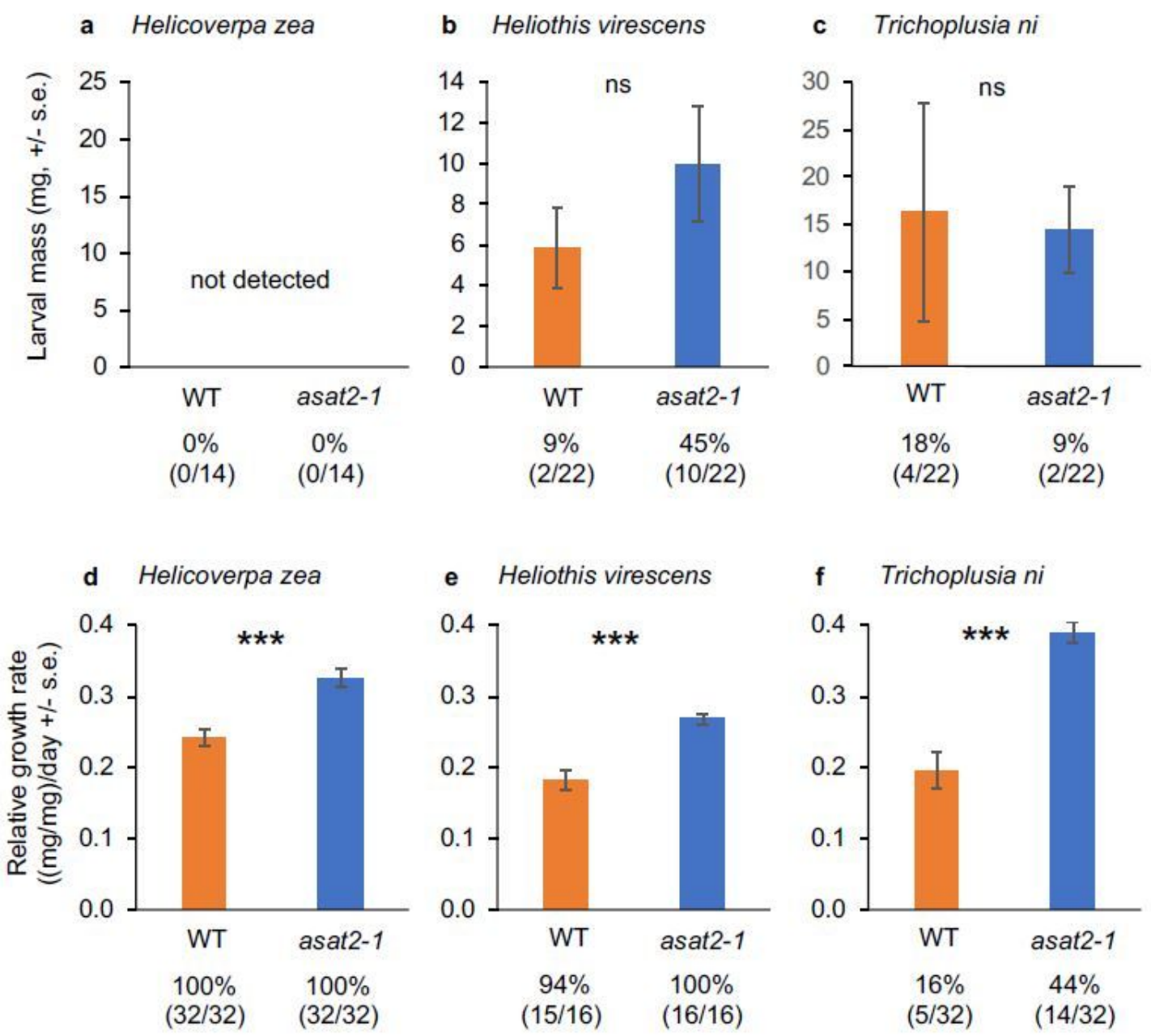

Figure 7

Caterpillar bioassays on wildtype (WT) and asat2-1 mutant Nicotiana benthamiana. (a, b, c) Larval mass of surviving Helicoverpa zea, Heliothis virescens, and Trichoplusia ni 10 days after being placed on plants as neonates. (d, e, f) Relative growth rate of surviving H. zea, H. virescens, and T. ni on wildtype and asat2-1 plants. Insects were raised for five days on artificial diet, prior to 7 days of feeding on N. benthamiana. Percent survival (number of surviving insects/number of total insects) is shown below each figure. Mean +/- s.e. ,***p < 0.001, t-test; ns: no significant difference (P > 0.05).

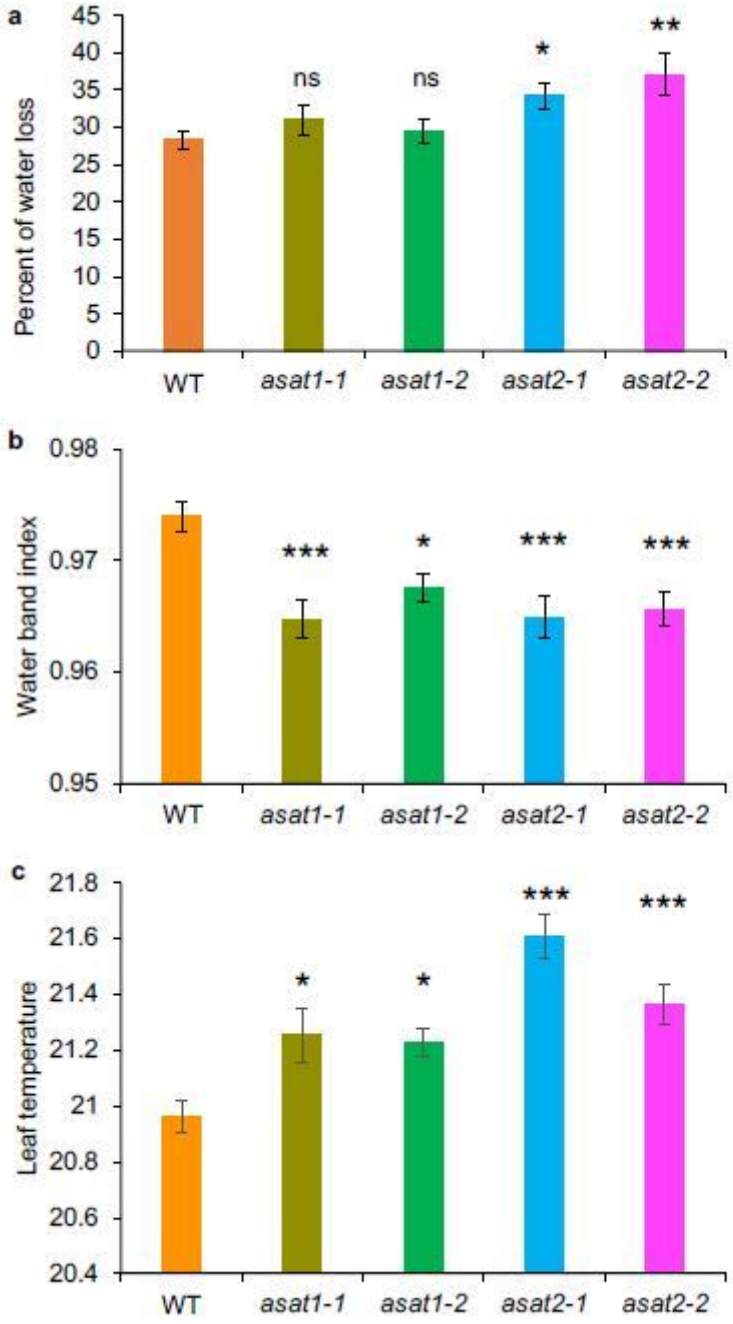

Figure 8

Water loss and leaf temperature of wildtype (WT), asat1, and asat2 Nicotiana benthamiana. (a) Percent of water loss from detached leaves in 24 hours, mean +/- s.e. of n = 15. (b) Leaf water content measured by the water band index from hyperspectral imaging , mean +/- s.e. of n = 20. (c) Leaf temperatures from leaves of different plant genotypes, mean +/- s.e. of n = 20. ns = no significant difference, *p < 0.05, **p < 0.01, ***p < 0.001, Dunnett's test relative to wildtype control.

Supplementary Files

This is a list of supplementary files associated with this preprint. Click to download.

- SupplementaryFigures.pdf
- ASATTableS1SolASATs.xlsx
- ASATTableS2proteinsequences.docx
- ASATTableS3rawdata.xlsx
- ASATTableS4gRNAsPrimers.xlsx